

EXPERIMENTAL INVESTIGATION OF COMPOSITE STRUCTURES DURING DYNAMIC IMPACT

S. Engel^(1,2), C. Boegle⁽²⁾, J. Majamaeki⁽²⁾, D.H.-J.A. Lukaszewicz^(2,3,*), F. Moeller⁽²⁾

(1) *PhD Student, TU Bergakademie Freiberg, Akademiestraße 6, D- 09596 Freiberg*

(2) *BMW AG, Research and Innovation Centre, Knorrstraße 147, D-80788 Munich*

(3) *Honorary Member of Staff, ACCIS, University of Bristol, Queen's Building, University Walk, BS8 1TR, Bristol*

(*) *Corresponding author: dirk.lukaszewicz@bmw.de*

Keywords: Braiding, Carbon-Fibre, Crash, Energy Absorption

Abstract

Lightweight and robust components with superior crash performance may result in significant weight reductions in automotive body-in-white (BIW) structures, which may improve the sustainability of future cars. Key-components for crashworthiness during a front crash are the axial members of the motor mount, which can take up a large proportion of the impact energy. Here we study the dynamics impact response of such mounts manufactured using triaxial-braiding of carbon fibre for several different material and geometry configurations.

1 Introduction

Reducing carbon-dioxide emissions of a car during its life cycle is the main challenge of the automotive industry in the 21st century. Fuel consumption during use generates the majority of these carbon-dioxide emissions and is thus one of the most promising areas for future improvements. Since the fuel consumption for a given car is proportional to the car weight weight reductions are desirable to further reduce fuel consumption. Simultaneously, requirements for passenger safety are constantly increasing, generally resulting in additional weight for the vehicle structure. One way to meet mass-saving and passenger safety requirements at the same time is to replace common steel-structures with novel carbon-fibre-reinforced ones, which may possess superior mechanical properties and energy absorption [1], yielding a significant weight saving potential. In a front crash, the kinetic energy of the vehicle has to be dissipated in the vehicle structure to protect the passengers. The plastic deformation of the engine mounts is one of the main means of energy dissipation in current car-structures. Several studies have demonstrated that the specific energy-absorption (SEA), which is the absorbed energy per unit weight of material of composite structures under axial loading, is superior to metals [2]. However, the mechanisms during composite failure are entirely different from metals and a novel understanding of these phenomena is required to effectively design vehicle structures that yield weight savings while meeting passenger safety requirements. The effect of cross-sectional shape and corner radii on SEA was studied by Palanivelu et al. [3], Mamalis et al. [4] and Deleo et al. [5]. Square and rectangular shapes were found to absorb 20% to 50% less energy, respectively, compared to round specimens

[6], [7], [8]. It was argued that this was due to the utilisation of the more regular stress-distribution in specimens with round cross-section. Feraboli et al. [9] thus studied rectangular structures with corner-/radii and demonstrated that radii could increase energy absorption. Jacob et al. [10] showed that specific energy absorption scaled with the ultimate compressive strength of a material and it was shown that composites with higher strength yielded higher energy absorption. However, this correlation was only valid as long as the failure mode was unchanged and changes in failure mode, for example due to changes in thickness this can reduce energy absorption significantly [11], [12]. There are several known factors that can change the failure mode. The influence of laminate architecture, such as fibre orientation, fibre volume fraction and layer thickness on energy absorption capability was studied by Lavoie and Kellas [13] and Hamada et al. [14]. The main finding was the pronounced effect of interlaminar fracture toughness on energy absorption and fracture mode, respectively. This was also observed for braided and woven materials where the in-plane properties were degraded by fibre ondulation, but showed a higher energy absorption capability due to their increased interlaminar fracture toughness as reported by Kim, Yoon and Shin [15] and Saito et al. [1]. Other parameters that can affect energy absorption are the fibre and matrix properties [16], [15], trigger geometry [10], [17], [3], [18], strain rate [19], [20], [21], [22] and temperature [23], [24], [25]. To conclude, there are several parameters known to influence the specific energy absorption of composite structures. However, little work has been done studying their interaction to understand failure of composite structures in different modes. In the current investigation this is addressed by studying the structural response of a dynamical axial compressed profile with rectangular cross-section. Geometrical parameters are varied as well as layup configuration to understand the impact of these variables in a unified manner for loading conditions found in automotive crash.

2 Experimental Procedure

2.1 Sample manufacture

From the literature, a subset of parameters was identified as most relevant to axial crush performance. These were corner radius, filler fibre fraction, number of layers and aspect ratio. The base specimen was 140mm by 100mm with a 20mm corner radius and consisted of 3 layers of braided material with 56% of fibres in $\pm 45^\circ$ and 44% of fibres in 0° direction. Several sets of different samples were thus manufactured having all these variables incorporated, see Table 1. In total 34 samples were manufactured for dynamic axial testing. Braiding was performed onto a foam core. The filler yarns were 50k carbon fibres while the braiding yarns were carbon fibres in 12k and 24k rovings. The different fibre-types were necessary to be able to alter the fraction of fibres in axial and transverse direction within the desired range. After braiding the specimens were wrapped in peel ply and then infused with epoxy resin and hardener using low-pressure resin-transfer moulding (RTM). After infusion

Table 1: Sample configurations for dynamic axial impact testing.

| Parameter | | - | 0 | + |
|--------------------|------|----------|----------|----------|
| Corner radius | [mm] | 15 | 20 | 25 |
| UD-Volume fraction | [%] | 28 | 44 | 61 |
| Braid layers | [-] | 2 | 3 | 4 |
| Aspect ratio | [-] | 1:2 | 1:1.4 | 1:1.08 |

the specimens were cured at 60°C for 4 hours. Then the core and peel ply were removed and the specimens were tempered at 95°C for 4 hours to fully cure all specimens. All specimens had a nominal fibre volume fraction of 50% and this was later checked by weighing the specimens after braiding, infusion and just prior to testing. The last weight was used to calculate the SEA of the crushed specimen length. The measured fibre volume fraction was $50.18\% \pm 1.70\%$ (by fibre volume) for all specimens. Lastly, the samples were machined to produce a chamfer trigger for crushing and to further prepare them for testing on a component crash test setup.

2.2 Testing Procedure

For testing each specimen was glued into a grooved base plate, which was additionally wrapped with room temperature curing glass-epoxy cloth. The base plate was then mounted into the test setup. Test conditions were varied for the samples depending on the expected energy absorption. The test speed was held constant at 8.2 m/s while the mass of the impactor was varied to obtain a reasonable crush length. The test consisted of accelerating the impactor to the desired speed and impacting the braided carbon structure axially, until the entire kinetic energy imparted by the impactor was absorbed through fragmentation and destruction of the specimen, see Figure 1a) and b). During testing the axial force as a function of time was recorded at the base plate. Further, high-speed imaging was used to correlate the measured force-time curve to specific failure modes. The velocity of the impactor was measured using optical devices.

3 Results

3.1 Experimental Results

The tested configurations and respective responses, peak force, mean force and crush length of the tests are summarised in Table 2 together with the weight-based performance metric SEA and the crush force efficiency (CFE), the latter being the ratio between the measured maximum and mean force for the component. In the case of the peak force, mean force and

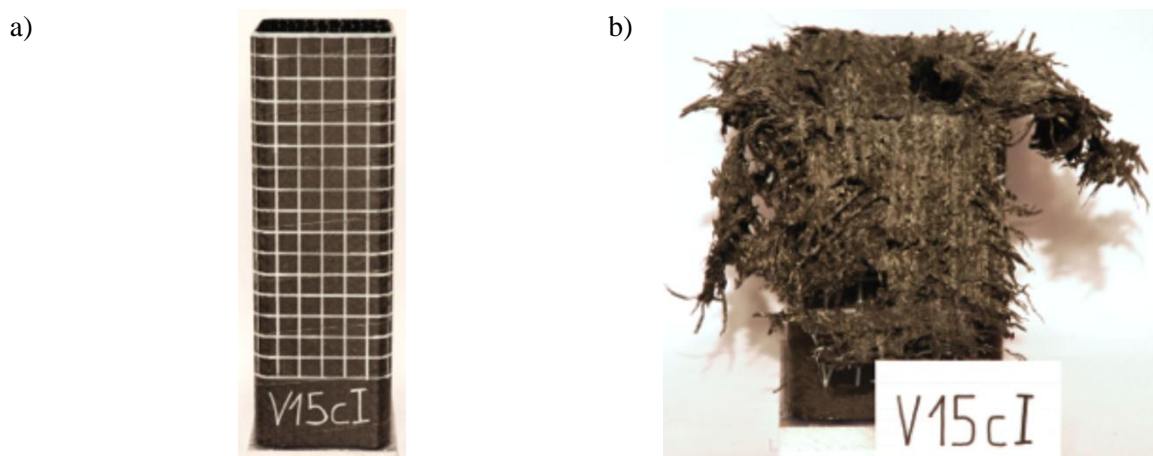


Figure 1: Example of a braided carbon composite structure a) prior to testing and b) after testing.

Table 2: Overview of the tested sample configurations, test conditions and respective results.

| Test # | Corner Radius [mm] | UD-Fraction [%] | Braid Layers [-] | Aspect Ratio [-] | Peak Force [-] | Mean Force [-] | Crush Length [mm] | SEA [kJ/kg] | CFE [%] |
|--------|--------------------|-----------------|------------------|------------------|----------------|----------------|-------------------|-------------|---------|
| V01 | 15 | 28 | 2 | 1:2 | 0.5 | 0.5 | 1.2 | 26.2 | 27.6 |
| V02 | 25 | 28 | 2 | 1:2 | 0.5 | 0.5 | 1.0 | 27.7 | 30.0 |
| V03 | 15 | 61 | 2 | 1:2 | 0.6 | 0.5 | 1.0 | 29.6 | 24.1 |
| V04 | 25 | 61 | 2 | 1:2 | 0.6 | 0.6 | 0.9 | 34.3 | 27.7 |
| V05 | 15 | 28 | 4 | 1:2 | 0.9 | 1.1 | 0.9 | 29.4 | 33.1 |
| V06 | 25 | 28 | 4 | 1:2 | 1.0 | 1.1 | 0.9 | 30.5 | 32.7 |
| V07 | 15 | 61 | 4 | 1:2 | 1.2 | 1.2 | 1.2 | 35.8 | 27.3 |
| V08 | 25 | 61 | 4 | 1:2 | 1.3 | 1.3 | 1.0 | 39.9 | 29.7 |
| V09 | 15 | 28 | 2 | 1:1.08 | 0.7 | 0.5 | 1.3 | 20.2 | 19.4 |
| V10 | 25 | 28 | 2 | 1:1.08 | 0.7 | 0.6 | 1.1 | 23.3 | 22.5 |
| V11 | 15 | 61 | 2 | 1:1.08 | 0.8 | 0.5 | 1.2 | 24.7 | 19.6 |
| V12 | 25 | 61 | 2 | 1:1.08 | 0.9 | 0.7 | 1.2 | 30.9 | 22.3 |
| V13 | 15 | 28 | 4 | 1:1.08 | 1.5 | 1.5 | 0.9 | 30.8 | 28.0 |
| V14 | 25 | 28 | 4 | 1:1.08 | 1.5 | 1.6 | 0.9 | 32.3 | 29.6 |
| V15 | 15 | 61 | 4 | 1:1.08 | 1.5 | 1.7 | 0.8 | 38.9 | 32.1 |
| V16 | 25 | 61 | 4 | 1:1.08 | 1.5 | 1.6 | 0.9 | 36.8 | 30.8 |
| V00 | 20 | 44 | 3 | 1:1.4 | 1.4 | 1.5 | 0.7 | 37.9 | 31.1 |

crushed length the data were normalised with respect to the mean. In all cases the reported results are the average of two individual tests. Initially, models were developed for correlating sample configurations and SEA and CFE and this is discussed in the following.

3.2 Model development and analysis

To develop an understanding of the interaction between the tested configurations the data were fitted with a second-order analytical model containing interaction terms for each of the possible parameter combinations, see Equation 1.

$$y = \beta_0 + \sum_{j=1}^k \beta_j x_j + \sum_{i < j}^k \sum_{j=2}^k \beta_{ij} x_i x_j \quad (1)$$

where y is the predicted response, such as peak force or crush length, x are the input variables, such as corner radius or aspect ratio, β are the fit coefficients and i, j, k are index variables. This model was developed for both the SEA and CFE results. The fitted Response Surfaces from the model function given in Equation 1 are shown in Figure 2a) – f) for the Specific Energy Absorption (SEA) and in Figure 3a) – f) for the Crush Force Efficiency (CFE). The R^2 for the full fitted model is 93% for the CFE and 87% for the SEA. The remaining variability in the data is expected to be due to the aforementioned scatter in fibre volume fraction between individual specimens.

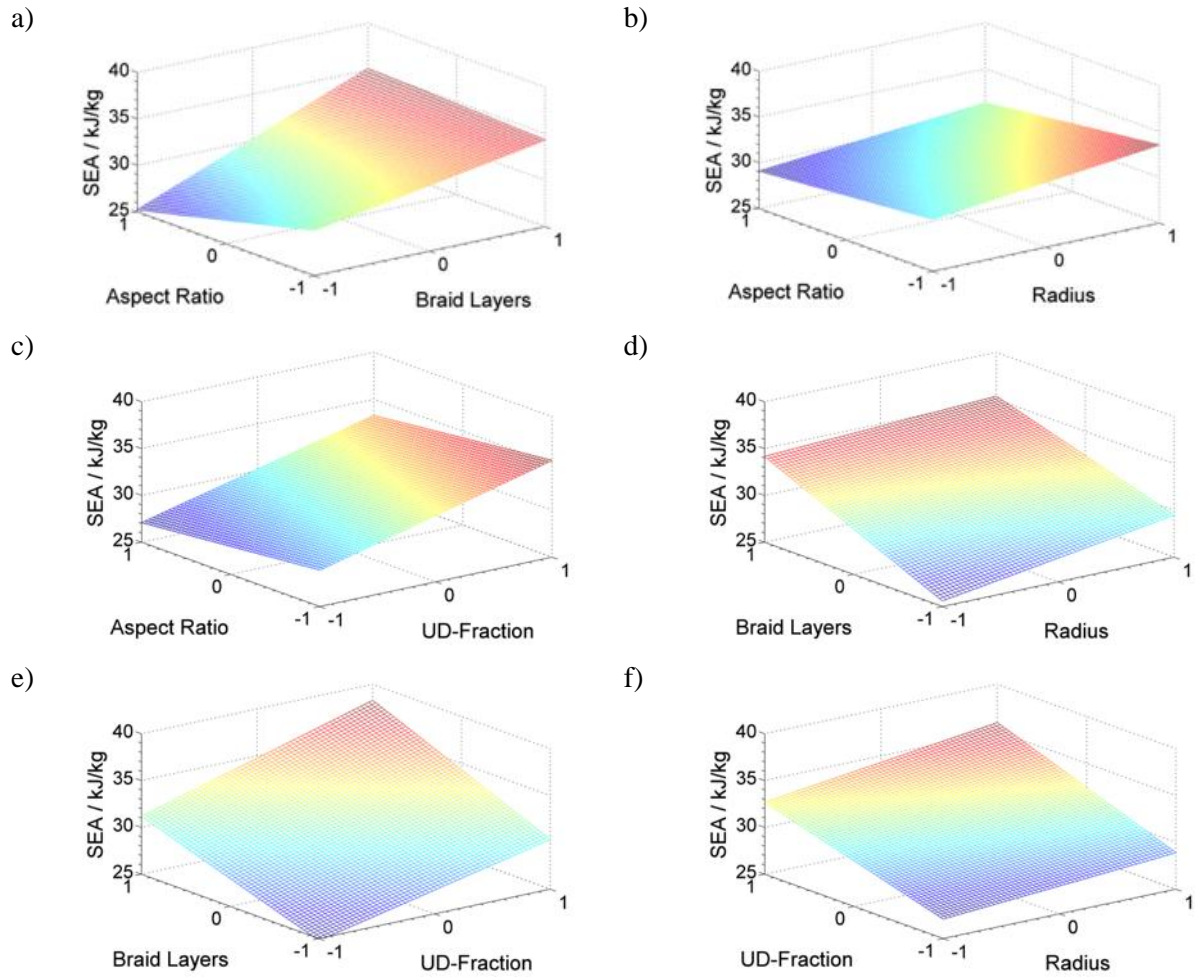


Figure 2a) – f): Response surfaces (RS) for the SEA fitted to the experimental data.

4 Discussion

A careful analysis of the data and a comparison to previously published results for comparable composite structures [26] [27] [28] shows that the SEA and CFE results reported here are significantly lower (31.1kJ/kg compared to 51kJ/kg) than previously reported [26]. However, while the results reported here were obtained for dynamically loaded specimens, typical results reported in the literature were obtained using quasi-static loading and it has been demonstrated by Karbhari and Haller [27] that this can account for the reduction in SEA and CFE. The response surfaces for the SEA show that the most promising drivers to increase the SEA are the number of layers as well as the UD-Fraction of the specimens. To understand the main mechanisms for the changes in SEA and CFE the coefficients of determination for the individual variables were calculated as well, according to Equation (2).

$$r^2 = \left[\frac{\sum_{i=1}^n (X_i - \bar{X}) (Y_i - \bar{Y})}{\sqrt{\sum_{i=1}^n (X_i - \bar{X})^2} \sqrt{\sum_{i=1}^n (Y_i - \bar{Y})^2}} \right]^2 \quad (2)$$

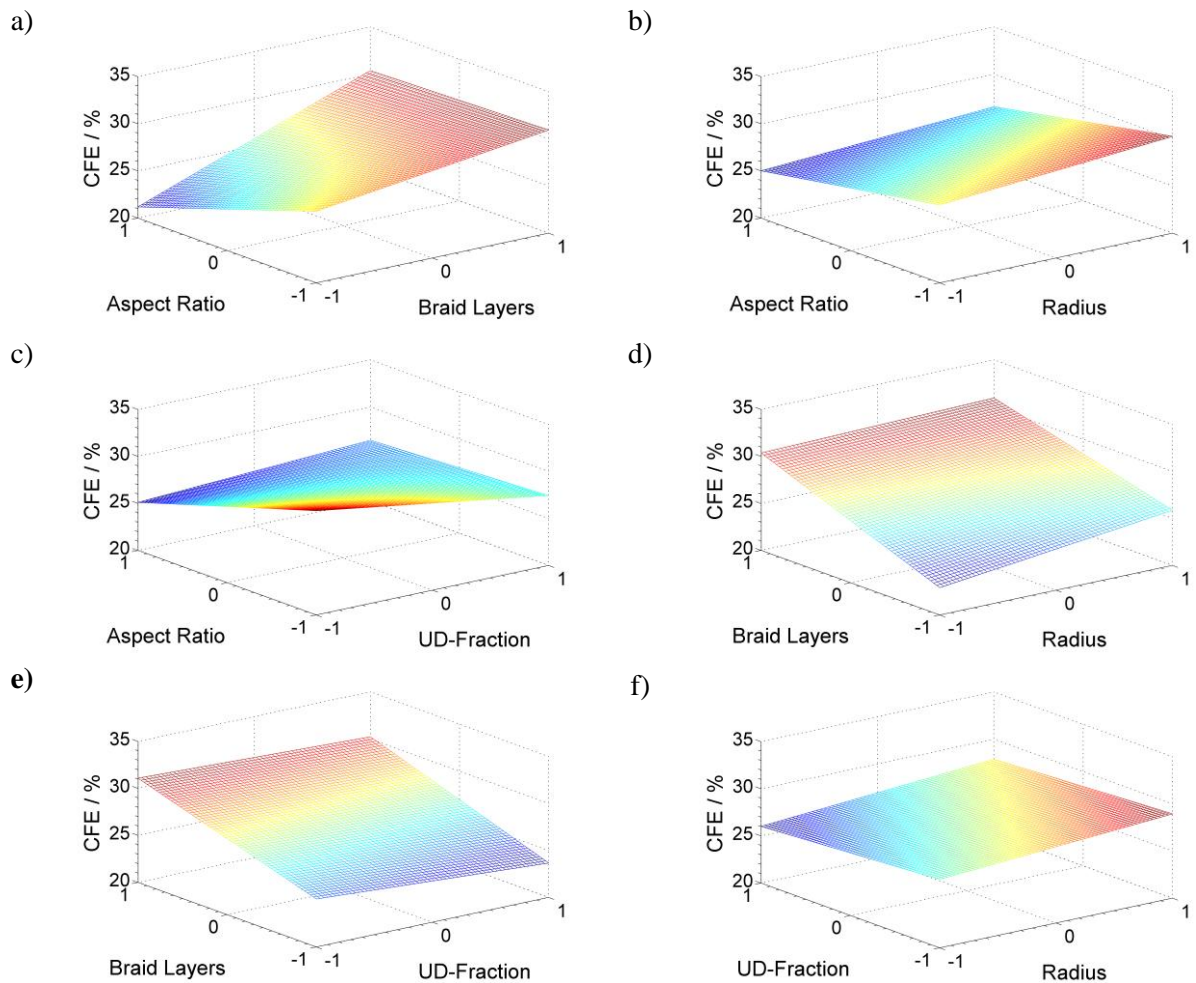


Figure 3a) – f): Response surfaces (RS) for the CFE fitted to the experimental data.

with r^2 being the square of Pearson's correlation coefficient, X_i and Y_i the respective variables, such as Radius and CFE. These are shown in Figure 4a) and Figure 4b). Since round specimens have generally been reported to yield higher energy absorption than rectangular specimens, it was expected that specimens with an aspect ratio closer to one and high corner radii would improve SEA. While this is indeed the case, the aspect ratio and corner radii have a surprisingly small effect on the SEA. Similarly, the CFE scales with the number of braid layers, however it is rather insensitive to all other variables. Interestingly, specimens with a low aspect ratio and UD-Fraction are found to yield improved CFE's. This may either lead to the conclusion that the CFE is governed by the material microstructure or by the trigger geometry. The trigger depends on the cross-sectional shape of the specimen and for square cross-sections 'tulip' trigger have been reported to be more effective for dynamic loading, as shown by Palanivelu et al. [3]. This implies that a chamfer trigger which is commonly used in quasi-static testing of round geometries is not suitable for dynamic loading of square structures and the variables that govern effective trigger geometries in dynamic loading will have to be studied further.

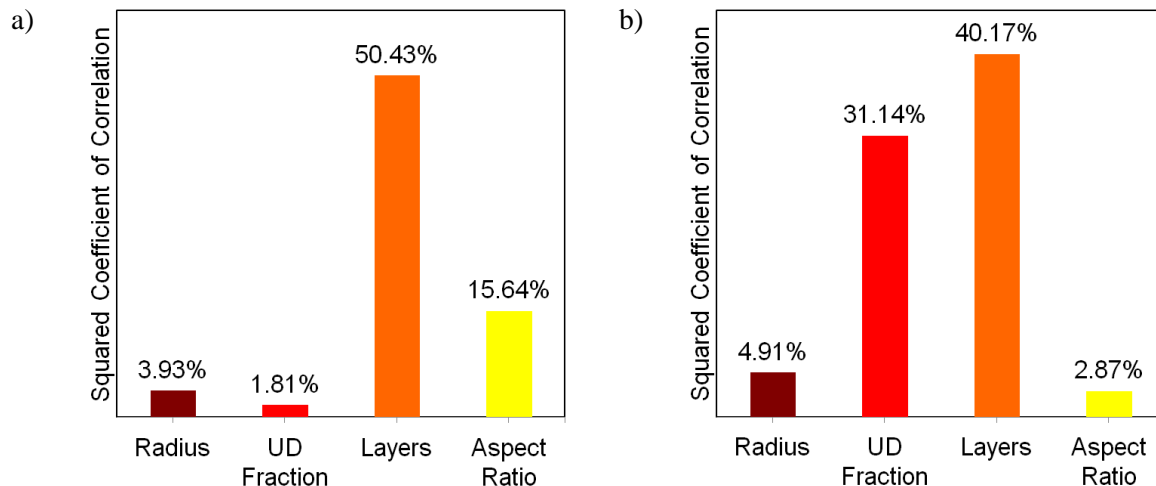


Figure 4: Coefficients of determination for a) the CFE and b) the SEA of rectangular composite beams during dynamic axial impact.

5 Further Work

Further work will be aimed at correlating structural variables, such as moment of inertia of a structure, as well as properties governed by microstructure and manufacturing, such as the compressive strength, with the SEA and CFE. Different material systems and layup architectures will be studied as well to develop a simple analytical tool that may be used to approximate the theoretical performance of energy absorbing structures in the early design-phase of a vehicle.

Acknowledgements

We would like to thank BMW Group (Munich, Germany) for funding this research. Further we are indebted to TTI (Stuttgart, Germany) for manufacturing of the specimens and Fraunhofer EMI (Freiburg, Germany) for the use of their test facilities.

References

- [1] Saito H., Chirwa E.C, Inai R., Hamada H.: Energy absorption of braiding pultrusion process composite rods. *Compos Struct* **55**/4, 407-417 (2002)
- [2] Bisagni C.: Experimental investigation of the collapse modes and energy absorption characteristics of composite tubes. *Int J Crashworthines* **14**/4, 365-378 (2009)
- [3] Palanivelu S.R., Paepegem W., Degrieck J., Ackeren J., Kakogiannis D., Hemelrijck D., Wastiels J., Vantomme J.: Experimental study on the axial crushing behaviour of pultruded composite tubes. *Polym Test* **29**/2, 224-234 (2010)
- [4] Mamalis A.G., Manolacos D.E., Ioannidis M.B., Papapostolou D.P.: On the response of thin-walled CFRP composite tubular components subjected to static and dynamic axial compressive loading: experimental. *Compos Struct* **69**/4, 407-420 (2005)
- [5] Deleo F., Wade B., Feraboli P., Rassaian M.: Crashworthiness of composite structures: experiment and simulation. In: *AIAA - 50th Structures, Dynamics and Materials Conference*. (2009)
- [6] Kindervater M. C.: Energy absorption of composites as an aspect of aircraft structural crash resistance. In: *Fourth European Conference on Composite Materials*. (1990)

- [7] Mamalis G. A., Manolakos E. D., Demosthenous A. G., Ioannidis B. M.: The static and dynamic axial crumbling of thin-walled fibreglass composite square tubes. *Composites Part B: Engineering* **28/4**, 439-451 (1997)
- [8] Mamalis A.G., Yuan Y.B., Viegelaahn G.L.: Collapse of thin-wall composite sections subjected to high speed axial loading. *Int. J. Vehicle Design* **13/5-6**, 564 (1992)
- [9] Feraboli P., Wade B., Deleo F., Rassaian M.: Crush energy absorption of composite channel section specimens. *Compos Part A* **40/8**, 1248-1256 (2009)
- [10] Jacob G.C., Fellers J.F., Simunovic S., Starbuck J.M.: Energy Absorption in Polymer Composites for Automotive Crashworthiness. *J Compos Mater* **36/7**, 813-850 (2002)
- [11] Hamada H., Ramakrishna S.: Scaling effects in the energy absorption of carbon-fiber/PEEK composite tubes. *Compos Sci Technol* **55/3**, 211-221 (1995)
- [12] Thornton P.H., Harwood J.J., Beardmore P.: Fiber-reinforced plastic composites for energy absorption purposes. *Composites Science and Technology* **24/4**, 275-298 (1985)
- [13] Lavoie A. J., Kellas S.: Dynamic crush tests of energy-absorbing laminated composite plates. *Composites Part A: Applied Science and Manufacturing* **27/6**, 467-475 (1996)
- [14] Hamada H., Kameo K., Sakaguchi M., Saito H., Iwamoto M.: Energy absorption properties of braided composite rods. *Composites Science and Technology* **60/5**, 723-729 (2000)
- [15] Kim J.-S., Yoon H.-J., Shin K.-B.: A study on crushing behaviors of composite circular tubes with different reinforcing fibers. *Int J Impact Eng* **38/4**, 198-207 (2011)
- [16] Farley G.L.: Energy absorption of composite material and structures. In: *Proceedings of the 43rd American Helicopter Society Annual Forum*. (1987)
- [17] Ghasemnejad H., Blackman B.R.K., Hadavinia H., Sudall B.: Experimental studies on fracture characterisation and energy absorption of GFRP composite box structures. *Compos Struct* **88/2**, 253-261 (2009)
- [18] Feraboli P.: Development of a Modified Flat-plate Test Specimen and Fixture for Composite Materials Crush Energy Absorption. *J Compos Mater* **43/19**, 1967-1990 (2009)
- [19] AL-Zubaidy H., Zhao x.-L., Al-Mihaidi R.: Mechanical Behaviour of Normal Modulus Carbon Fibre Reinforced Polymer (CFRP) and Epoxy under Impact Tensile Loads. *Procedia Engineering* **10/0**, 2453-2458 (2011)
- [20] Focht R. J., Woldesenbet E., Vinson R. J.: High Strain Rate Properties of IM7/977-3 Graphite/Epoxy Composites. In: *39th Structures, Structural Dynamics, and Materials Conference*. (1998)
- [21] Hou J.P., Ruiz C.: Measurement of the properties of woven CFRP T300/914 at different strain rates. *Compos Sci Technol* **60/15**, 2829-2834 (2000)
- [22] Hsiao M. H., Daniel M. I.: Strain rate behavior of composite materials. *Composites Part B* **29/5**, 521-533 (1998)
- [23] Asp L.E.: The effects of moisture and temperature on the interlaminar delamination toughness of a carbon/epoxy composite. *Compos Sci Technol* **58/6**, 967-977 (1998)
- [24] Mamalis G. A., Robinson M., Manolakos E. D., Demosthenous A. G., Ioannidis B. M., Carruthers J.: Crashworthy capability of composite material structures. *Compos Struct* **37/2**, 109-134 (1997)
- [25] Numata D., Ohtani K., Anyoji M., Takayama K., Togami K., Sun M.: HVI tests on CFRP laminates at low temperature. *International Journal of Impact Engineering* **35/12**, 1695-1701 (2008)
- [26] Chiu C.H., Tsai K.-H., Huang W.J.: Crush-failure modes of 2D triaxially braided hybrid composite tubes. *Compos Sci Technol* **59/**, 1713-1723 (1999)
- [27] Karbhari M. V., Haller E. J.: Rate and architecture effects on progressive crush of braided tubes. *Composite Structures* **43/2**, 93-108 (1998)
- [28] Farley L. Gary: The Effects of Crushing Speed on the Energy-Absorption Capability of Composite Tubes. *J Compos Mater* **25/**, 1314-1329 (1991)